Energy Migration in Novel pH-Triggered Self-Assembled β-Sheet Ribbons

Veysel Kayser, David A. Turton, Amalia Aggeli, Andrew Beevers,
Gavin D. Reid, and Godfrey S. Beddard*

*Contribution from the Department of Chemistry and Centre for Chemical Dynamics,
University of Leeds, Leeds, LS2 9JT, UK*

Received March 27, 2003; E-mail: godfrey.beddard@chem.leeds.ac.uk

Abstract: Energy migration between tryptophan residues has been experimentally demonstrated in self-assembled peptide tapes. Each peptide contains 11 amino acids with a Trp at position 6. The peptide self-assembly is pH-sensitive and forms amphiphilic tapes, which further stack in ribbons (double tapes) and fibrils in water depending on the concentration. Fluorescence spectra, quenching, and anisotropy experiments showed that when the pH is lowered from 9 to 2, the peptide self-assembly buries the tryptophan in a hydrophobic and restricted environment in the interior of stable ribbons as expected on the basis of the peptide design. These fluorescence data support directly and for the first time the presence of such ribbons which are characterized by a highly packed and stable hydrophobic interior. In common with Trp in many proteins, fluorescence lifetimes are nonexponential, but the average lifetime is shorter at low pH, possibly due to quenching with neighboring Phe residues. Unexpectedly, time-resolved fluorescence anisotropy does not change significantly with self-assembly when in water. In highly viscous sucrose—water mixtures, the anisotropy decay at low pH was largely unchanged compared to that in water, whereas at high pH, the anisotropy decay increased significantly. We concluded that depolarization at low pH was not due to rotational diffusion but mainly due to energy migration between adjacent tryptophan residues. This was supported by a master equation kinetic model of Trp—Trp energy migration, which showed that the simulated and experimental results are in good agreement, although on average only three Trp residues were visited before emission.

Background

Polypeptides have an intrinsic ability for self-assembly. This is demonstrated for example by a variety of biological and designed proteins that self-assemble into twisted amyloid β-sheet polymers typically 5–10 nm in diameter,[1–8] e.g., characterizing Alzheimer's and prion diseases and as seen with the de novo β-sandwich protein betabellin 15D.[9]

Exploiting the intrinsic self-assembling property of peptides, we have recently shown[10–13] that it is possible to form a hierarchy of new, controllable, and well-defined polymeric structures. In particular oligomeric peptides can be rationally designed to adopt a β-strand conformation and to self-assemble one after the other in one dimension to form elongated, one-molecule-thick, polymeric β-sheet tapes in appropriate solution conditions. The tapes can further stack in pairs to form two-molecule-thick double tapes or ribbons; several ribbons can stack to form fibrils, and pairs of fibrils can entwine edge-to-edge to form fibers.

Within a tape, and hence in the higher order structures, the amino acid side-chains along the peptide β-strands alternate up and down relative to the plane defined by the intermolecular, hydrogen-bond network forming the β-sheet peptide backbone. If side-chains at positions 1, 3, 5, etc. are on the upper side of the tape, then side-chains at 2, 4, 6, etc. will be on the opposite side Figure 1A. Self-assembly is driven not only by these numerous intermolecular peptide backbone hydrogen bonds but also by side-chain to side-chain interactions.[10–13] The underlying β-sheet lattice imposes fixed distances between specific side-chains on adjacent β-strands, depending on whether the peptides arrange in a parallel or in an antiparallel manner. Clearly, the overall dimensions of the tapes depends on the number of

* Author for correspondence.
(1) Fink, A. L. *Folding Des.* **1998**, *3*, R9 – R23.
(2) Sunde, M.; Blake, C. F. *Q. Rev. Biophys.* **1998**, *31*, 1–39.
(3) Kirschner, D. A.; Elliott-Bryant, R.; Szumowski, K. E.; Gonnerman, W. A.; Kindy, M. S.; Sipe, J. D.; Cathcart, E. S. *J. Struct. Biol.* **1998**, *124*, 88–98.
(4) Seilheimer, B.; Bohrmann, B.; Bondolfi, L.; Muller, F.; Stuber, D.; Dobeli, H. *J. Struct. Biol.* **1997**, *119*, 59–71.
(5) Jimenez, J.; Guijarro, J.; Orlova, E.; Zurdo, J.; Dobson, C.; Sunde, M.; Saibil, H. R. *EMBO J.* **1999**, 815–821.
(6) West, M. W.; Wang, W.; Patterson, J.; Mancias, J. D.; Beasley, J. R.; H., H. M. *Proc. Natl. Acad. Sci. U.S.A.* **1999**, *96*, 11211–11216.
(7) Fandrich, M.; Fletcher, M. A.; Dobson, C. M. *Nature* **2001**, *410*, 165–166.
(8) Marini, D. M.; Hwang, W.; Lauffenburger, D. A.; Zhang, S.; Kamm, R. D. *Nano Lett.* **2002**, *2*, 295–299.
(9) Lim, A.; Saderolm, M. J.; Makhov, A. M.; Kroll, M.; Yan, Y.; Perera, L.; Griffith, J. D.; Erickson, B. W. *Protein Sci.* **1998**, *7*, 1545–1554.
(10) Aggeli, A.; Bell, M.; Boden, N.; Keen, J. N.; McLeish, T. C. B.; Nyrkova, I.; Radford, S. E.; Semenov, A. *J. Mater. Chem.* **1997**, *7*, 1135–1145.
(11) Aggeli, A.; Nyrkova, I. A.; Bell, M.; Harding, R.; Carrick, L.; McLeish, T. C. B.; Semenov, A. N.; Boden, N. *Proc. Natl. Acad. Sci. U.S.A.* **2001**, *98*, 11857–11862.
(12) Nyrkova, I. A.; Semenov, A. N.; Aggeli, A.; Boden, N. *Eur. Phys. J. B* **2000**, *17*, 481–497.
(13) Nyrkova, I. A.; Semenov, A. N.; Aggeli, A.; Bell, M.; Boden, N.; McLeish, T. C. B. *Eur. Phys. J. B* **2000**, *17*, 499–503.

β-strands that laterally self-assemble and on the peptide chain length and nature of amino acid side chains, but typically each β-strand contributes ~0.47 nm to the length and 0.5–1.5 nm to the thickness of a tape depending on the amino acids used; in our peptide, this value is 1.2 nm. The number of amino acids in a β-strand multiplied by 0.335 nm gives the tape width.

All of these hierarchical structures, tapes, double tapes (or ribbons), fibrils, and fibers are twisted due to the intrinsic chirality of the peptide molecules. A mathematical model has been developed that describes this self-assembly process of chiral rodlike molecules.[11,14,15] The model's parameters determine (1) the critical peptide concentration (c^*) necessary for onset of self-assembly, (2) the fraction of peptide molecules in monomeric and self-assembled states, (3) the type of polymer formed, and (4) the equilibrium average polymer size and the size distribution as a function of peptide concentration in solution.

Most interestingly, the magnitudes of these parameters can be controlled not only by peptide design but also by a variety of external triggers. The latter opens up a self-assembly route to produce peptide polymers that can be controlled by external stimuli, and we have recently produced a series of de novo peptides whose self-assembly is controlled by pH.[16]

These self-assembling peptides are good model systems for gaining insight into the intrinsic properties of the β-sheet structure in biology. Equally exciting is the prospect of using peptide self-assembly as a route to novel, smart, nanostructured biopolymers whose chemical, bioactive, mechanical, and structural properties can be controlled by peptide design.

Tryptophan fluorescence is widely used to study structure and dynamics of peptides and proteins, and for this purpose the tryptophanyl residue has several advantages. Of the three naturally occurring fluorescent amino acids, it has by far the highest radiative rate and fluorescence yield and its fluorescence is strongly influenced by its environment. The emission maximum roughly correlates with the degree of solvent exposure and varies from ~308 to 315 nm for the buried Trp in azurin to ~355 nm for the water-exposed Trp in glucagon. This will only be true provided that energy transfer between Trp residues in multi-Trp proteins is absent. In multi-Trp proteins Trp–Trp energy transfer[17] can occur if the Forster transfer distance R_0, variously estimated to range from 0.7 to 1.6 nm depending upon the environment,[18–23] is comparable to or larger than Trp to Trp separation. In multi-Trp proteins, it is usually assumed that the fluorescence properties are additive because Trp residues are assumed to be electronically isolated from one another. Energy migration between Trp residues will change this view, however, and still remains one of the least studied problems in protein fluorescence spectroscopy.

The two lowest electronic transitions of the indole, designated ^1L_a and ^1L_b, are close in energy, and both contribute to the absorption spectrum. Fluorescence is thought to arise from the ^1L_a state, which is strongly influenced by the environment and red-shifted in polar solvents; the ^1L_b is comparatively insensitive.[24] Quantum calculations indicate that upon excitation, electron density shifts from the pyrrole to the benzene ring when the ^1L_a state is formed. This means that positive charge near to the benzene or negative charge near to the pyrrole end of the indole will lower the energy and lead to red-shifted absorption and vice versa if charges are exchanged. The size of the shift varies with the size of the Coulomb interaction, which in turn depends proportionally upon the relative orientation of the charge relative to the Trp and inversely with their separation.

In this paper, we describe for the first time the excited-state properties of the Trp residue of a designed pH-responsive self-assembling peptide P_{11}-4, in its monomeric and aggregated β-sheet states in solution as well as Trp–Trp energy migration. The peptide P_{11}-4 has the primary structure Ace–Gln–Gln–Arg–Phe–Glu–Trp–Glu–Phe–Glu–Gln–Gln–NH$_2$ and was designed to form β-sheet tapes and higher-order aggregates in water; see Figure 1. At pH > 7.5, the intermolecular electrostatic repulsions between the three negatively charged Glu side-chains result in a monomeric random coil state in a wide range of peptide concentrations up to several mM.[16] At pH < 7.5, due to the progressive neutralization of the negative charges, P_{11}-4 spontaneously self-assembles into antiparallel β-sheet aggregates, Figure 1. On the basis of its amphiphilic primary structure, P_{11}-4 is expected to self-assemble into amphiphilic β-sheet tapes, i.e., having two distinct sides, one predominantly hydrophobic (Gln2, Phe4, Trp6, Phe8, Gln10) and one hydrophilic (Gln1, Arg3, Glu5, Glu7, Glu9, Gln11). Such tapes will have intermolecular side-chain interactions Gln to Gln, a salt bridge between Arg3 and Glu9, and π–π stacking of the aromatic side-chains. It is further expected that in water, the tapes will prefer to stack in pairs to form ribbons, to shield their hydrophobic sides from water, Figure 1C,D.

Methods

Peptide production was carried out using standard solid-phase peptide synthesis protocol.[10] The HPLC-purified peptide was checked by analytical HPLC, mass spectrometry, and amino acid analysis. The mass spectrum showed only one main peak corresponding to the molecular weight of P_{11}-4 equal to 1596 Da. Amino acid analysis confirmed the expected composition of the peptide.

A solution of P_{11}-4 (5 mg/mL, equal to ~3.3 mM) at pH 2 in H$_3$PO$_4$ was prepared, vortexed, sonicated, and immediately diluted to micromolar concentrations while optically isotropic. The diluted samples were left at 20 °C in an incubator for 2 days before they were used. In the same way, a pH 9 solution was prepared with NaOH and treated similarly to that at pH 2. Solutions for quenching experiments were prepared as described above, except that NaCl was added to keep the ionic strength the same in each solution. N-Acetyl L-tryptophanamide (NATA) and acrylamide were purchased from Aldrich and Fisher Scientific, respectively, and used as received.

Fluorescence spectra and relative yields were measured with a FluoroMax-3 (Jobin Yvon-Horiba) fluorimeter, and excited-state lifetimes were measured by picosecond, single-photon counting using a synchronously pumped, Nd:YAG/cavity-dumped, dye-laser with a Hamamatsu microchannel-plate detector and Becker & Hickl detection electronics. Fluorescence decays were measured at 54.7° and analyzed

(14) Chothia, C. *J. Mol. Biol.* **1973**, *75*, 295–302.
(15) Salemme, F. R. *Prog. Biophys. Mol. Biol.* **1983**, *42*, 95–133.
(16) Agelli, A.; Bell, M.; Carrick, L.; Fishwick, C. W.; Harding, R.; Mawer, P.; Radford, S. E.; Strong, A.; Boden, N. *J. Am. Chem. Soc.* **2003**, *125*, 9619–9628.
(17) Förster, T. *Annal. Phys.* **1948**, *6*, 55–75.
(18) Lakowicz, J. R. *Principles of Fluorescence Spectroscopy*, 2nd ed.; Kluwer Academic/Plenum: New York, 1999.
(19) Willaert, K.; Loewenthal, R.; Sancho, J.; Froeyen, M.; Fersht, A.; Engelborghs, Y. *Biochemistry* **1992**, *31*, 711–716.
(20) Weber, G. *Biochem. J.* **1960**, *75*, 335–345.
(21) Lakowicz, J. R.; Cherek, H.; Gryczynski, I.; Joshi, N.; Johnson, M. L. *Biophys. J.* **1987**, *51*, 755–768.
(22) Alfimova, E. Y.; Likhtenstein, G. I. *Mol. Biol. (Moscow)* **1976**, *8*, 127–179.
(23) Wu, P.; Brand, L. *Anal. Biochem.* **1994**, *33*, 1–13.

(24) Vivian, J. T.; Callis, P. R. *Biophys. J.* **2001**, *80*, 2093–2109.
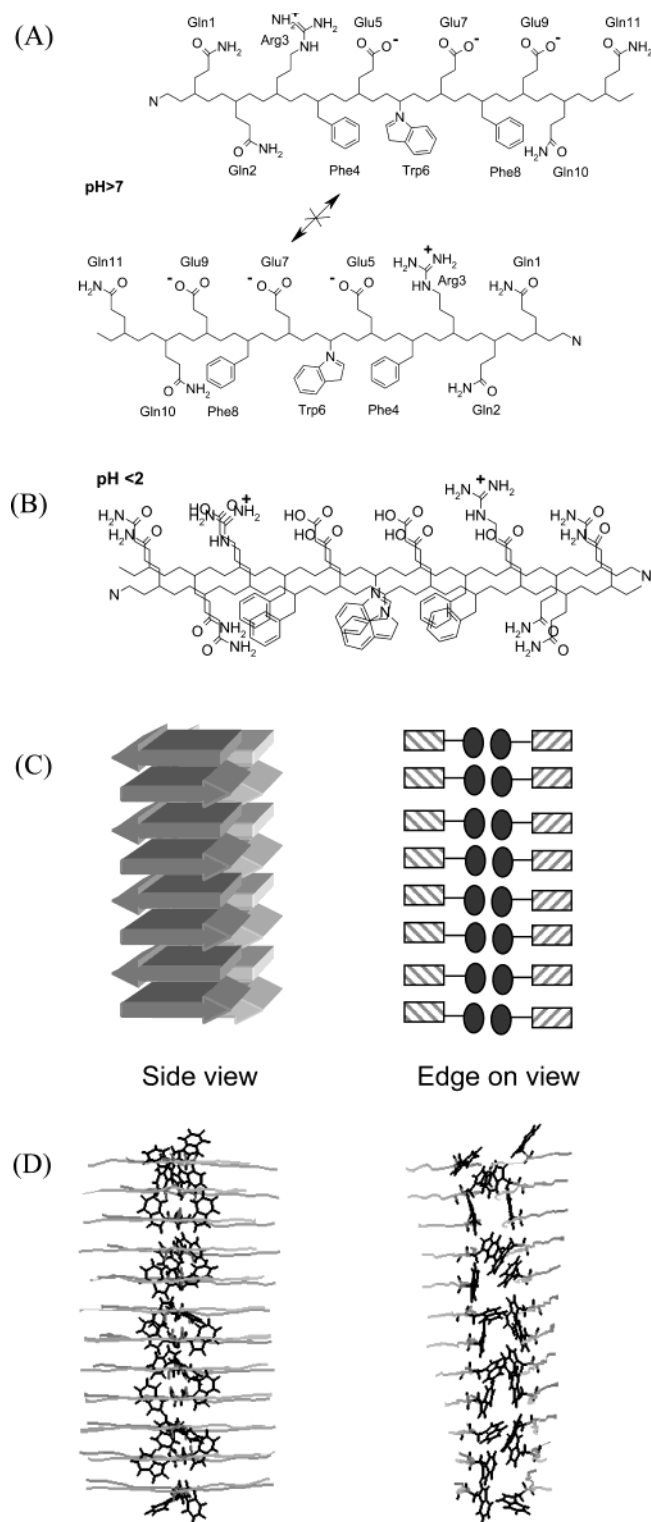
Figure 1. (A) Side view schematic of arrangement of two peptides at pH ≥ 7 where charges on Glu prevent self-assembly and (B) side view of two peptides self-assembled at pH ≤ 2. (C) Highly schematic view of a self-assembled double tape, or ribbon. Arrows denote individual peptides, the circles denote Trp residues. The left-hand diagram is a side-view; the right-hand diagram is an edge on view obtained by rotating the left view by 90°. (D) More detailed side and edge-on view as in C of part of an optimized model of a double tape or ribbon. Only the Trp residues are shown explicitly and are buried inside the ribbon.

using the Marquardt–Levenberg algorithm as a sum of n single exponential functions using the minimum number of terms to fit the data. Typically, $n = 3$ and convolution with the detector response was

performed where necessary. Excitation was at 295 nm and detection at >300 nm selected with filters. The anisotropy was calculated from measurements with vertical and horizontal polarizers and analyzed with the following equation

$$r(t) = \sum_{i=1..2} r_{i0}\exp(-t/\phi_i) + r_\infty$$

In the particular case of a chromophore performing constrained motion in a protein or membrane then[25]

$$r(t) = [(r_0 - r_\infty)\exp(-t/\phi_r) + r_\infty]\exp(-t/\phi_B).$$

The initial anisotropy is r_0, and r_∞ is the anisotropy remaining at long periods of time; ϕ_B is the lifetime for the whole body rotational motion of the peptide, which is assumed to be describable by a single parameter, and ϕ_r is the local "wobbling in a cone" motion of the Trp.[25] If the absorption and emission dipoles are parallel and lie along the symmetry axis of the probe's rotation, then $r(\infty)/r(0) = [1/2\cos(\theta_m)(1 + \cos(\theta_m))]^2$, where θ_m is the maximum cone semiangle of the hypothetical cone in which the probe diffuses, and if the absorption and emission dipoles are perpendicular, then $r(\infty)/r(0) = [1/2(1 - \cos^2(\theta_m))]^2$, where θ_m is now the minimum cone angle, the maximum being π radians.

The overlap integral[17,26,27] for Trp–Trp Förster transfer $J = \int\epsilon(v)\phi(v)v^{-4}\,dv$ was estimated from the overlap of the measured absorption spectrum, $\epsilon(v)$ in dm^3 mol^{-1} cm^{-1}, and the area normalized emission spectrum $\phi(v)$, where v represents wavenumbers. The transfer distance R_0 is conventionally defined using $R_0^6 = (2/3)CJQ$ where $C = 9000\ln(10)/(128\pi^5 n^4 N)$, and Q is the fluorescence quantum yield, 0.14, in the absence of quenchers; N is Avogadro's number, and n the refractive index. At pH 9, n was taken to be that of water, 1.33, but at pH 2, where the Trp is buried in a hydrophobic environment, $n = 1.44$. R_0 is in the range reported for other proteins,[19,28–30] $R_0 = 0.67$ nm at pH 9 and 1.15 nm at pH 2. Light scattering, particularly in the pH 2 samples introduces some uncertainty in the R_0 values because this scattering background had to be removed. The value at pH 2 where the background scattering was greatest is likely to be an overestimate, although clearly greater than that at pH 9: the absorption spectrum at both pHs is similar, but the pH 2 emission is blue-shifted to peak at 312 nm compared to 355 nm at pH 9. The errors on R_0 values are estimated as (+0.05, −0.1) nm. The rate coefficient for dipole–dipole (Forster) energy transfer between two molecules i and j is

$$k_{ij} = \frac{3}{2}k_f\chi_{ij}^2\left(\frac{R_0}{R_{ij}}\right)^6$$

where k_f is the mean fluorescence decay rate in the absence of any quencher. The orientational parameter χ is given by $\chi_{ij} = \bar{s}_i\bar{s}_j - 3(\bar{s}_i\bar{r})(\bar{s}_j\bar{r})$, where $\bar{s}$ is a unit vector along the molecular dipole and $\bar{r}$ a unit vector between their centers on molecules i and j. By using the above equations, we have implicitly assumed the Trp molecules to be point dipoles; while more sophisticated models can be used, we considered that these would not be justified at present. The structures of the peptide tapes and ribbons were constructed in HyperChem and simulated in TINKER[31,32] using the AMBER force field. Molecular

(25) Kinosita, K.; Kawato, S.; Ikegami, A. *Biophys. J.* **1977**, *20*, 289–305.
(26) Förster, T. *Discuss. Faraday Soc.* **1959**, *27*, 7.
(27) Förster, T. In *Modern Quantum Chemistry*; Sinanoglu, O., Ed.; Academic Press: New York, 1965; Vol. 3, pp 93–137.
(28) Hennecke, J.; Sillen, A.; Huber-Wunderlich, M.; Engelborghs, Y.; Glockshuber, R. *Biochemistry* **1997**, *36*, 6.
(29) Engelborghs, Y.; Fersht, A. In *Topics in Fluorescence Spectroscopy*; Lakowicz, J. R., Ed.; Kluwer Academic: Dorchrecht, 2002; Vol. 6, pp 83–100.
(30) Maartensson, L.-G.; Jonasson, P.; Freskgaard, P.-O.; Svensson, M.; Carlsson, U.; Jonsson, B.-H. *Biochemistry* **1995**, *34*, 1734–1743.
(31) Ponder, J. W.; Richards, F. M. *J. Comput. Chem.* **1987**, *8*, 1016–1024.
(32) Ponder, J. http://dasher.wustl.edu/tinker (accessed 2001).

Table 1. Decay Parameters for Trp Fluorescence of P_{11}-4 in Monomeric Random Coil State at pH 9 and in Self-Assembled Ribbon State at pH 2[a]

	τ_1 (ns)	f_1	τ_2 (ns)	f_2	τ_3 (ns)	f_3
pH 9	1.38	0.46	3.18	0.52	6.94	0.02
pH 2	0.86	0.58	2.94	0.37	6.85	0.05

[a] τ are lifetimes, and f are fractions with lifetime τ, $I(t) = \sum_{i=1..3} f_i \exp(-t/\tau_i)$.

dynamics (MD) simulations were run for 100 ps in steps of 2 fs using a modified Beeman algorithm.[8,33,34] A fuller account is described elsewhere.[35] The main use of the molecular dynamics calculation in this paper was to obtain the positions of Trp molecules. The solvent water molecules were simulated using a continuum dielectric model. The starting structure was a flat segment of either a tape or a ribbon consisting of 24 peptide molecules; using charges as determined by the pH of the solution, only under pH 2 conditions did the calculations show that self-assembly occurs. The Trp molecules in the ribbons were observed to be almost immobile on the time scale of the simulation. They can be approximately grouped into three classes with deviation ∼5° about their mean angles as measured relative to the vector defined by the N atoms on Glu 5 to Glu 7.

Results & Discussion

The MD simulation shows that the Trp 6 of P_{11}-4 in the ribbon state is separated from its nearest neighbor by a range of distances varying from 0.4 to 0.75 nm, and all next-nearest neighbors lie within 0.85 nm. The molecular modeling calculations suggest that the tryptophans are buried in the hydrophobic core of the ribbon at pH 2, and this is confirmed from the fluorescence spectrum, which shows a spectrum peaking at 312 nm; by contrast, the monomeric random coil P_{11}-4 at pH 9 has a spectrum peaking at 355 nm. The emission peak of P_{11}-4 at pH 2 is similar to the emission peak of the buried Trp in azurin[36] at 312 nm, whereas the emission peak of P_{11}-4 at pH 9 is reminiscent of those of the water-exposed Trp in melittin or glucagon, which have random coils with little α-helix content and emission peaks at ∼345 and ∼355 nm, respectively.

Excited-State Quenching. The fluorescence lifetimes at pH 2 and 9 are fitted to the sum of three exponentials with lifetimes τ and fractional components f, Table 1, with average values $\langle \tau \rangle = 1.87$ and 2.44 ns, respectively. At pH 9, P_{11}-4 has values that are similar to those observed in other short peptide chains,[37−39] for example, in melittin,[40] where $\tau_1 = 3.24$ ns ($f_1 = 0.64$), $\tau_2 = 0.64$ ns ($f_2 = 0.36$), and $\langle \tau \rangle = 2.3$ ns at pH 9.

It has been shown that Trp fluorescence is quenched by excited state charge-transfer to nearby acceptor groups. Multiple single-exponential lifetimes are observed, provided that distinct C^α−C^β bond conformers are present during the excited-state lifetime and that these conformers are quenched at different

rates. The rate of quenching depends on the redox properties of the acceptors, their separation, eq 1, and orientation to the Trp. The peptide group and other electrophiles such as amino groups and to a lesser extent −CH_3 and −COO^- are all potential quenchers.[41,42] A single exponential fluorescence decay is almost never to be expected, as the conditions required for this to occur are hardly ever achieved. These are either that only one conformer is present in only one type of environment and that this is very long lived compared to the Trp radiative lifetime or that if many conformers are present that they rapidly interconvert, again compared to the radiative lifetime. The model predicts that when a Trp is buried in a ribbon, whether a shorter or longer excited-state lifetime will be observed, compared to that of a peptide in monomeric random coil state, will also depend on which C^α−C^β conformers can be realized and on the availability of nearby quenchers.

Using the MD model of the self-assembled ribbon at low pH, we can examine the separation of Trp from possible quenchers. The indole groups of the Trp6 form a hydrophobic region on the interior of the ribbon together with the phenyl groups of Phe4 and Phe8 with which they are in close contact. The aromatic groups such as in Phe have recently been shown to quench Trp fluorescence via a transient H bonding interaction with the indole NH group. The indole group is not forced into such close contact with the Phe side-chains in the monomeric random coil peptide state at pH 9. Thus, this difference in Trp− Phe interaction could explain the slightly shorter average fluorescence lifetime at pH 2 in comparison to that at pH 9, which is due mainly to τ_1 decreasing from 1.38 to 0.86 ns.[43] The glutamic acids (Glu5 and Glu7), which are on either side of the Trp6 in the primary structure, contain a potential quencher in the −COOH/−COO^- groups of their side chains, but these groups are both on the outside of the ribbon (i.e., line the hydrophilic sides of the tapes), in contact with the water and too far away from Trp6 (0.9−1.2 nm) to quench effectively. The closest peptide groups to the Trp6 side chains are the −CONH− of the adjacent Glu5 and Glu7, which are only 0.4 to 0.5 nm away. In the ribbons the Trp are constrained by packing to lie largely over the peptide backbone but in a range of different orientations. The closeness of the peptide bonds to the Trp side chains could also rationalize the shorter fluorescence lifetime observed in the ribbons at pH 2 vs the monomeric random coil peptide at pH 9, where the same interaction can occur but the Trp is not constrained and thus spends less time in a favorable orientation for quenching. If the charge-transfer coupling is of the point-monopole, point-dipole type, the interaction has the form $2q\Delta\bar{\mu}\bar{r}/r^3$ and thus depends strongly on orientation and separation. The heterogeneity of orientations in the ribbons and of orientations and separation in the single peptides qualitatively explains the observed emission decays.

Stern−Volmer quenching using acrylamide as a quencher was also used to determine whether the Trp is buried in the hydrophobic core of the ribbons at pH 2. In a simple quenching process, the fluorescence yield F at quencher concentration $[Q]$ and that at zero quencher F_0 is related to the second-order rate constant for quenching, k_q, and the fluorescence lifetime τ_0 as $F_0/F = 1 + k_q\tau_0[Q]$. As both self-assembled and single peptides

(33) Beeman, D. J. *J. Comput. Phys.* **1976**, *20*, 130−139.
(34) Hwang, W.; Marini, D. M.; Kamm, R. D.; Zhang, S. J. *J. Chem. Phys.* **2003**, *118*, 389−397.
(35) Fishwick, C. W. G.; Beevers, A. J.; Aggeli, A.; Carrick, L. M.; Whitehouse, C. D.; Boden, N. *Nano Lett.* **2003**, *3*, 1475−1479.
(36) Petrich, J. W.; Longworth, J. W.; Fleming, G. R. *Biochemistry* **1987**, *26*, 2711−2722.
(37) Chen, L. X. Q.; Petrich, J. W.; Fleming, G. R.; Perico, A. *Chem. Phys. Lett.* **1987**, *139*, 55−61.
(38) Tran, C. D.; Beddard, G. S.; Osborne, A. D. *Biochim. Biophys. Acta* **1982**, *709*, 256−264.
(39) Adams, P.; Chen, Y.; Ma, K.; Zagorski, M. G.; Sönnichsen, F. D.; McLaughlin, M. L.; Barkley, M. D. *J. Am. Chem. Soc* **2002**, *124*, 9278− 9286.
(40) Tran, C. D.; Beddard, G. S. *Eur. Biophys. J.* **1985**, *13*, 59−64.

(41) Petrich, J. W.; Chang, M. C.; Mcdonald, D. B.; Fleming, G. R. *J. Am. Chem. Soc.* **1983**, *105*, 3824−3832.
(42) Beddard, G. S.; Tran, C. D. *Eur. Biophys. J.* **1985**, *11*, 243−248.
(43) Nanda, V.; Brand, L. *Proteins: Struct. Funct. Genet.* **2000**, *40*, 112−125.
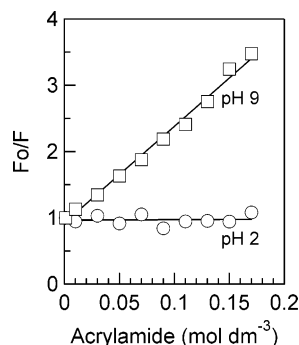
Figure 2. Stern−Volmer plot of Trp quenching by acrylamide in β-sheet ribbons at pH 2 (circles) and in monomeric random coil peptides at pH 9 (squares). The solid lines are linear least-squares fits to the data. See text for details.

can coexist in an amount depending upon pH, the ratio of fluorescence yields at a different pH[44] can be used to determine the pK, which is 4.8 ± 0.5, indicating that protonating Glu triggers self-assembly because this residue has a pK of 4.3 and because it is the only residue present with a pK between 4 and 6.[45]

At pH 9, the measured value of k_q is 5.98×10^9 M^{-1} s^{-1}, but this value is approximately 160 times smaller, 3.8×10^7 M^{-1} s^{-1}, at pH 2, Figure 2. These two extreme values mimic the rate constants observed for glucagon, 3.7×10^9 M^{-1} s^{-1} and azurin, 5×10^7 M^{-1} s^{-1}.[46] As acrylamide is water-soluble it is energetically unfavorable for it to enter into the hydrophobic interior of the ribbon. The pH 2 result confirms that the Trp is here buried in a stable hydrophobic core and its fluorescence is not affected by the presence of the acrylamide quencher in the aqueous phase. By contrast, the rate constant for NATA quenching at pH 2 is 3.7×10^9 M^{-1} s^{-1} and 5.4×10^9 M^{-1} s^{-1} at pH 9, which are within error the same as literature values.[47,48] The quenching behavior of Trp is well-known for proteins with buried vs exposed Trp residues.[46] The smallest separation of the Trp in the interior of the ribbon at pH 2 to the quencher in the aqueous phase is estimated as 0.5 nm. As quenching is by electron transfer, if we assume that k_q at pH 9 is the value at contact, which means that the centers of the molecules are at a separation, σ, then the rate constant k at pH 2 can be estimated from the Marcus equation

$$k = k_0 \exp(-\beta[r - \sigma]) = k_q \exp(-\beta r) \qquad (1)$$

where r is the quencher−Trp separation in the ribbon state at pH 2 and β has a value of approximately 14 nm^{-1} in proteins.[49,50] With this value of β and a separation $r \geq 0.38$ nm, then $k \leq 0.005 k_q$.

A more detailed examination at pH 9 reveals a nonlinear Stern−Volmer relationship, but this does not change the main conclusion, which is that at pH 9, the Trp is exposed to water but is buried at pH 2. From the pH 2 curve in Figure 2, we concluded that close to 100% of the peptide must be in a self-

(44) Beddard, G. S. In preparation.
(45) Stryer, L. *Biochemistry*, 3rd ed.; W. H. Freeman and Co.: New York, 1988.
(46) Eftink, M. R.; Ghiron, C. A. *Biochemistry* **1976**, *15*, 672−680.
(47) Eftink, M. R.; Ghiron, C. A. *Biochemistry* **1997**, *16*, 55546−5551.
(48) Weber, J.; Senior, A. E. *Biochemistry* **2000**, *39*, 5287−5294.
(49) Moser, C. C.; Keske, J. M.; Warncke, K.; Farid, R. S.; Dutton, P. L. *Nature* **1992**, *355*, 796−802.
(50) Farid, R. S.; Moser, C. C.; Dutton, P. L. *Curr. Opin. Struct. Biol.* **1993**, *3*(2), 225−233.

Table 2. Anisotropy Decay Parameters of Trp of P$_{11}$-4, Fitted with $r(t) = \sum_{i=1..2} r_{i0}\exp(-t/\phi_i) + r_\infty$

pH	r_∞	τ_1 (ps)	r_{10}	τ_2 (ps)	r_{20}
2 water	0.030	603	0.10	47.8	0.046
2 + sucrose	0.029	1032	0.079	41.7	0.063
9 water	0.00	596	0.138	35.4	0.048
9 + sucrose	0.0008	3003	0.120	65.6	0.063

assembled state at this pH, which means that the self-assembled peptides must be very stable with little measurable free peptide.

Fluorescence Anisotropy. Rotational diffusion of the whole peptide and local motion of the Trp are measured by the decay in fluorescence anisotropy. A similar effect can also be caused by energy transfer and energy migration even when no rotational motion is possible. In the monomeric peptides at pH 9, energy migration is clearly not possible, but could be in the ribbons, where many Trp are in close proximity, Figure 1B. To determine if this was the case, fluorescence lifetimes and anisotropy measurements were made at both pH 9 and 2 with a viscosity of 1 cP and in a sucrose−water mixture with a viscosity of 10.5 cP. The Trp fluorescence anisotropies at pH 2 and 9 in water are, coincidentally, very similar to one another, having an initial anisotropy $r_0 = 0.21$ and decaying to zero with lifetimes of 590 ± 20 ps and 35 ± 5 ps at pH 9, and $r_0 = 0.18$ and 600 ± 20 ps and 48 ± 5 ps at pH 2. However, the Trp fluorescence anisotropies in the more viscous sucrose−water solutions pH 2 and 9 are vastly different from one another at pH 9, being 65 ± 20 and 3000 ± 150 ps, and at pH 2 are much more similar to those in water at 40 ± 5 and 1000 ± 50 ps. We aim to show that the causes of these depolarizations are different under the two different pH conditions used. The longer component of the anisotropy from the single peptides at pH 9 in water or in the sucrose−water mixture is attributed to the whole body motion of the peptide, while the shorter component is due to local wobbling in a cone motion of the Trp.[25,51] If we suppose that one of the peptide molecules has the prolate geometry shown in Figure 1A, it has dimensions of approximately 3.9, 1.25, and 0.4 nm. Assuming that the larger of the two smaller dimensions defines the diameter, the reciprocal of the diffusion coefficients parallel, $1/D_\parallel$, and perpendicular, $1/D_\perp$, to the long axis are, in water, 1.1 and 3.6 ns, respectively; this leads to an anisotropy decay that has three exponential terms with rotational correlation times of $\phi_1 = 1/6D_\perp = 0.61$ ns, $\phi_2 = 1/(4D_\perp + 2D_\parallel) = 0.24$ ns and $\phi_3 = 1/(5D_\perp + D_\parallel) = 0.44$ ns. The pre-exponential terms depend on the angle of the Trp dipole to the long axis of the peptide.[52] At pH 9, molecular modeling indicates that the peptide geometry is a random coil but with some peptides folded. Estimating the average peptide geometry to have semi-axes of 1 and 0.75 nm, the reciprocal diffusion coefficients are $1/D_\parallel = 3.1$ and $1/D_\perp = 3.8$ ns and rotational correlation times are 0.63, 0.55, and 0.61 ns. It would seem reasonable, therefore, in view of the rough estimate of the shape and geometry of the peptide to ascribe the longer lifetime, ~0.6 ns, decay of the anisotropy to tumbling of the peptide; the shorter component is then due to local motion of the Trp.

When self-assembled, the structures are so big that no significant bulk motion could occur, which should depolarize

(51) Lipari, G.; Szabo, A. *Biophys. J.* **1980**, *30*, 489−506.
(52) Fleming, G. R. *Chemical Applications of Ultrafast Spectroscopy*; Oxford University Press: New York, 1986.
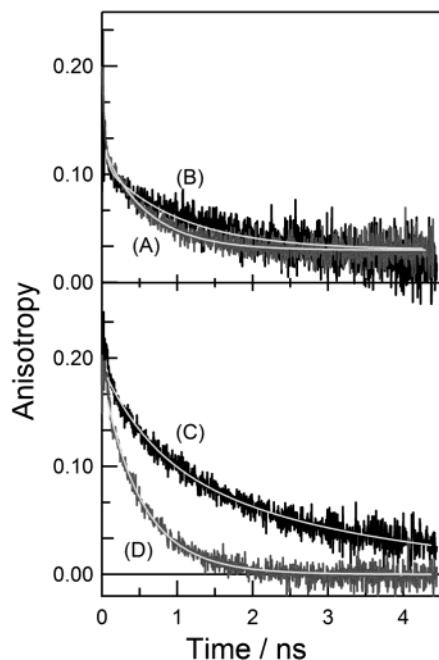
Figure 3. Experimental and calculated Trp anisotropy decays of P₁₁-4 in water at pH 2 (A) and pH 9 (D) and in sucrose−water mixtures at pH 2 (B) and pH 9 (C).

the fluorescence even in water. Depolarization does still occur, however, and this can have two causes: local motion as in the single peptide, or energy migration to other Trp via the very weak, dipole−dipole or Förster interaction. We first discuss whether local motion of the Trp caused depolarization.

The Trp in the ribbons is not exposed to solvent and is therefore not affected by the solvent viscosity. In wild-type azurin, a small protein containing a single buried Trp, fluorescence anisotropy measurements show that the Trp is highly confined and exhibits no local motion; only whole protein motion is observed.[36,53] Our simulations indicate that a similar situation occurs in the ribbons to that in azurin because the Trps are held in van der Waals contact with one another and with the two phenyl groups of adjacent Phe, by the intermolecular hydrogen bond interactions between peptide backbones, and between side-chains Gln2 and Gln10 that are responsible for tape formation. In the wobbling in a cone model of Kinosita et al.,[25,51] the ratio of r_∞ to r_0 is a measure of cone semiangle the local diffusive motion a chromophore can explore. At pH 9, $r_\infty/r_0 \approx 0$ and the cone semiangle approaches 90°, so that the indole group is unhindered in its motion in a hemisphere while attached to the peptide. When buried, the Trp anisotropy has the ratio $r_\infty/r_0 \approx 0.205$, and using the two limiting cases outlined in Method, the Trp dipole can undergo excursions in a cone with a semiangle from 0° up to 48° if the dipole is parallel to the figure axis or from 126 to 180° if the dipole is perpendicular to that axis. In either case, the anisotropy data indicates very considerable rotational motion if this is to be attributed to the cause of the depolarization. However, this type of motion is highly unlikely to be the cause of the depolarization for the reasons just given, and we consider energy migration to be a more realistic explanation.

(53) Giampiero, M.; Rosato, N.; Agrio, A. F. In *Topics in Fluorescence Spectroscopy*; Lakowicz, J. R., Ed.; Kluwer Academic: Dorchrecht, 2002; Vol. 6, pp 67−79.

Energy migration may be considered to be due to multiple, consecutive energy transfer steps, each one being in the weak-coupling limit, which treats a transfer as being due to dipole−dipole coupling. This mechanism does not depend on rotational motion to depolarize the emission but only upon relative orientation of donor and acceptor and their absorption and emission spectra (see Methods). These properties are essentially unaltered by adding sucrose to increase viscosity of the solution. As a test of our supposition that energy migration causes the anisotropy decay, energy migration was simulated using an MD structure of the peptide ribbon and a master equation to solve the kinetic equations. The rate coefficient for transfer, k_{ij}, from each Trp, i, to any other, j, in the ribbon was calculated using the experimentally determined overlap integral for Forster transfer. The fixed orientations and separations of the Trp dipoles were obtained from the MD simulation of a structure containing 96 peptide chains, and it was assumed that each molecule fluoresces with the same rate coefficient k_f. The fastest jump time between Trps is 2 ps when $R_0 = 1.2$ nm and 35 ps when $R_0 = 0.75$ nm; both are longer than relaxation times in the excited state, which means that steady state spectra can be validly used in calculating the overlap integral. The weak interactions and relatively large separations between Trp indicate that energy migration is a kinetic, i.e., proceeds via a series of discrete steps, rather than coherent process.

The kinetic equation for the population P of a molecule i is:

$$\frac{dP_i}{dt} = -P_i[k_f + \sum_{i \neq j} k_{ij}] + \sum_{j \neq i} P_j k_{ji} \qquad (2)$$

where k_f is the reciprocal of the measured fluorescence lifetime and k_{ij} the energy transfer rate coefficient between molecule i and j. These simultaneous equations can be solved by finding the eigenvalues and eigenvectors of the matrix M whose elements m_{ij} are

$$m_{ij} = -[k_f + \sum_l k_{lj}(1 - \delta_{lj})]\delta_{ij} + (1 - \delta_{ij})k_{ij} \qquad (3)$$

where δ is the Kronecker delta. The population at time t, is the vector $P(t)$ obtained by evaluating

$$P(t) = V^{-1}[\exp(\lambda t)]VP_0$$

where λ are the eigenvalues, which are formed into the diagonal matrix, $[\exp(\lambda t)]$, and V is the eigenvector matrix and V^{-1} its inverse. P_0 is a column vector of initial populations. Because all the molecules are assumed to be the same, in the absence of any contrary information, the Boltzmann factor on the rate coefficients is unity and $k_{ij} = k_{ji}$. Ensemble averaging was achieved by exciting each molecule in turn; for each molecule excited, the total population of all molecules was calculated as a function of time and the results were summed. The total fluorescence intensity as if detected in a vertical and horizontal direction after vertically polarized excitation was determined and used to calculate the anisotropy, $r(t) = (I_v - I_h)/(I_v + 2I_h)$. Different angles of the Trp emission dipole relative to the absorption dipole were tested. The transition dipole for the L_a state lies almost exactly along a line from the center of the molecule and through the N atom, and the L_b dipole lies
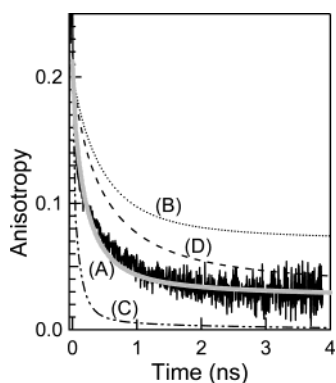
Figure 4. Measured anisotropy from P_{11}-4 ribbons at pH 2 in water and calculated (smooth line, A) from master equation with $Ro = 0.75$ nm and a dipole angle of 100°. The dotted line (B) is a calculation with the dipole angle set at 50° showing the lack of depolarization at long periods of time; the dashed line (C) with $Ro = 0.12$ nm and a dipole angle of 100°; and (D) the calculation with the same parameters as in A but with one jump to the nearest neighbor only. The simulated data was normalized to the peak of the experimental data.

approximately 92° anticlockwise to this dipole.[54,55] The energies of these two states are known to be close to one another, and usually fluorescence arises from the L_a transition; however, in very nonpolar solvents or hydrophobic environments, the fluorescence, which is structured and occurs at 310 to 320 nm, may be from the L_b state.[55] The initial anisotropy 0.22 predicts an angle of 36° between absorption and emission dipoles in accordance with experiment;[37-39] however, femtosecond up-conversion experiments[56] show that a rapid (~sub ps) dephasing occurs in the excited state and which, with resolution of only a few picoseconds, reduces the true anisotropy, which is 0.4 down the instrument-limited value reported here. An anisotropy of 0.4 means that the absorption and L_a emission dipoles are parallel to one another. In our simulations the best fit to the data was obtained with the larger range of angles $95 \pm 10°$, which suggests that in the self-assembled structures, the L_b excited state is emitting; this is consistent with the short emission wavelength. Figure 4 shows the experimental data at pH 2 together with simulations with an Ro value of 0.75 nm, which is also somewhat smaller than the value obtained from the absorption and emission spectra, 1.2 nm. The results shown in Figure 4C demonstrate that Ro as large as 1.2 nm cannot describe the data, as far too fast an initial anisotropy is present. The reason for the discrepancies between calculation and experiment is presumably due to the limited ability of the molecular mechanics simulations to produce a structure at a sufficient level of detail. When using fluorescence depolarization to study energy migration, there are two limiting cases to consider. First, if the dipoles are all aligned parallel to one another, even though migration might be occurring there is no depolarization and fluorescence anisotropy cannot measure migration. Conversely, provided that acceptor molecules are located at random around a donor, Galanin[57] has shown that the first step accounts for the majority of the depolarization even if migration subsequently occurs. The anisotropy caused by allowing only one energy-transfer step is shown in Figure 4D,

(54) Yamamoto, Y.; Tanaka, J. *Bull. Chem. Soc. Jpn.* **1972**, *45*, 1362−1366.
(55) Eftink, M. R. In *Methods of Biochemical Analysis*; Suelter, C. H., Ed.; Wiley: New York, 1991; Vol. 35, pp 127−205.
(56) Ruggerio, A. J.; Todd, D. C.; Fleming, G. R. *J. Am. Chem. Soc.* **1990**, *112*, 1003−1014.
(57) Galanin, M. D. *Trudy Fiz. Inst., Akad. Nauk S.S.S.R* **1950**, *5*, 339−386.

and clearly insufficient depolarization is produced to match the experimental data no matter what the dipole angle is.

The anisotropy for a range of dipole angles relative to the long axis of the indole group of Trp was also calculated while allowing multiple transfers, i.e., migration, to occur, eq 2. An example is shown in Figure 4B for a dipole angle of 50°, which shows that while some initial depolarization is occurring, the overall order of the Trp in the ribbons limits depolarization. Only when the angle is $95 \pm 10°$ are the calculated and experimental data in good agreement Figure 4A.

Finally, as a test of the method, energy migration in the protein penicillin acylase was simulated using the coordinates from the X-ray structure, Brookhaven Data Bank index 1GK9. This protein contains 28 Trp residues, but no significant energy migration was observed and the calculated anisotropy decayed 15 times slower than the fluorescence. This lack of energy transfer is confirmed by recent experimental data.[58]

The kinetic scheme in eq 2 allows us to calculate the mean square displacement of the excitation, as we have estimates of the Trp positions, and thereby estimate the diffusion coefficient for energy migration. The geometry of the double tape or ribbon is considered overall as being three-dimensional, Figure 1D, rather than simplified to two dimensions.

Initially the ensemble of excited molecules is far from equilibrium, and accordingly the mean square displacement $\langle R^2 \rangle$ must increase with time whatever the spatial arrangement of the Trp. In classical diffusion in a macroscopically homogeneous but microscopically disordered, three-dimensional ensemble, $\langle R^2 \rangle$ is given by the familiar Einstein formula

$$\langle R^2 \rangle = 6D_\infty t \tag{4}$$

where D_∞ is the steady state or limiting diffusion coefficient. Forster[17] has shown that if the transport process is by energy migration instead of molecular diffusion, the diffusion coefficient is given explicitly by

$$D_\infty = 2.81 k_f R_0^6 s^{4/3} \tag{5}$$

where s is the number density of chromophores. In calculating diffusion we shall assume that the excited molecules only undergo energy transfer and do not decay. In our model, the diffusion coefficient D_∞ was calculated using $D_\infty = 1/6n^2 \sum_{i,j} R_{ij}^2 k_{ij}$ for n molecules and where k_{ij} is the energy transfer rate constant between molecules i and j at a distance R_{ij}. Using different Ro values with our ribbon geometry, we found that the calculated $D_\infty \propto R_0^6$, and hence eq 5 is obeyed. We found agreement over at least 10 orders of magnitude, with $s = 0.052$ nm^{-3}, and this result justifies our use of a three-dimensional model rather than a two-dimensional model in which D_∞ would have a lower power dependence upon Ro. However, calculating $\langle R^2 \rangle$ as a function of time, we find that it increases less slowly than eq 4 would predict; perhaps this is not surprising, as this equation was derived to describe the random Brownian motion of molecules, not energy migration. Haan and Zwanzig[59] have from first principles described the energy migration between molecules distributed randomly in

(58) Ercelen, S.; Kazan, D.; Erarslan, A.; Demchenko, A. P. *Biophys. Chem.* **2001**, *90*, 203-217.
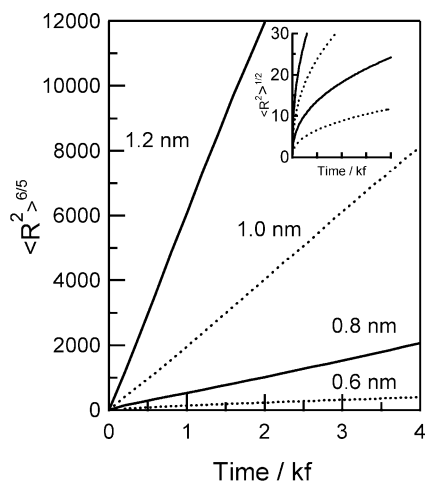(59) Haan, S. W.; Zwanzig, R. *J. Chem. Phys.* **1978**, *68*, 1879−1883.

Figure 5. Calculated displacement $\langle R^2 \rangle$ raised to the 6/5 power vs dimensionless time t/k_f, see eq 6. The R_0 values for the migration are shown. The inset shows an expanded view of the root-mean-square displacement for the same data over the same time range.

space and conjectured that

$$\langle R^2 \rangle \approx \frac{4\pi}{3} 2.975 s R_0^5 (k_f t)^{5/6} \qquad (6)$$

The limiting diffusion coefficient, however, is still given by an equation similar to eq 5 but with a constant of 2.19 instead of 2.81. When $R_0 < 1$ nm, we find that eq 6 describes the simulated data up to about four excited-state lifetimes, Figure 4. Diffusion at short times is often observed to follow a scaling law of the form $\langle R^2 \rangle \sim t^{2/d_w}$ which can describe diffusion on a fractal topology[60−62] when the dimension $d_w > 2$. In our case, the topology is not fractal, even though we have a $t^{5/6}$ time dependence and this is a result of the complicated diffusion equation rather than some underlying fractal nature of the ensemble.[62] From Figure 5, we can estimate the extent of migration at a given time using the R_0 value found to fit the experimental data in Figure 4. After a time $\langle \tau \rangle$, the mean fluorescence decay time, the energy has moved on average 0.13 nm, which means that it has also, on average, moved between three Trp molecules.

Conclusion

The photophysics of Trp in a new class of pH sensitive self-assembling peptides is consistent with behavior of Trp in other small proteins, and we observe that the excited state decay of Trp in a single peptide is nonexponential and explained by electron transfer from conformers to nearby groups. When self-assembled into double tapes (ribbons) of peptides at low pH,

the Trp is buried in a hydrophobic environment and produces a blue-shifted fluorescence spectrum similar to azurin. At pH 9, the peptides are not self-assembling and the Trp is free to undergo rotational diffusion. At pH 2, where self-assembly occurs, the fluorescence anisotropy decays in a manner similar to that at pH 9. Examining the simulated structure shows that the close packing of Trp residues with one another and with Phe restricts local rotational motion. However, as the fluorescence anisotropy tends toward zero within the excited state lifetime of the Trp, energy migration among Trp is the only reasonable explanation for this observation. A corollary to this is that the anisotropy cannot be used in this case to determine if the peptides are self-assembled. To confirm that energy migration is possible, the anisotropy decays were also simulated using a master equation, with rates given by the Forster, dipole−dipole model of energy transfer and which are in good agreement with the observed data. Calculation of the mean square displacement of the migration with time follows a 5/6 power law predicted by Haan and Zwanzig.

In general, as a self-assembled structure is vast compared to a single component from which it is composed, and if packing is such that local molecular rotation is restricted, fluorescence anisotropy is not expected to decay appreciably. In principle, it could be used as a measure of the rate and extent of self-assembly, particularly when the structure is still small enough that overall tumbling motion is comparable to the singlet (or triplet) excited state lifetime. However, it should also be generally true that, if energy transfer or migration is possible, changes in fluorescence anisotropy cannot be relied upon. An exception occurs if the chromophores are so arranged that their transition dipoles all point in the same direction. In this case, whether or not energy migration occurs, such a fixed spatial arrangement cannot change the fluorescence anisotropy; only molecular tumbling can do this. Other optical properties produced when chromophores are closely packed such as changes to the absorption spectrum, self-quenching of the excited states, charge transfer or electron-transfer reactions, excimer or exciplex emission, or accessibility to external quenchers, as is demonstrated here, have to be used.

(60) Sahimi, M. *Applications of Percolation Theory*; Taylor & Francis: London, 1994.
(61) Stauffer, D.; Aharony, A. *Introduction to Percolation Theory*, 2nd ed.; Taylor & Francis: London, 1994.
(62) Dewey, T. G. *Acc. Chem. Res.* **1992**, *25*, 195−200.